A Plasma Torch Model

B. Chinè
School of Materials Science and Engineering, Costa Rica Institute of Technology, Cartago, Costa Rica
P.O. Box 159-7050, Cartago, Costa Rica, bchine@itcr.ac.cr

Abstract:
Plasma torches are used in processing of materials and in energy industry for producing plasma. In this work we use the Plasma´s Equilibrium Discharge interface of Comsol Multiphysics® 5.1 to model a DC non- transferred arc plasma torch, under hypothesis of local thermodynamic equilibrium. The model of the plasma torch is implemented by also using the physics of CFD (Laminar flow), Heat Transfer (Heat transfer in fluids/solids) and AC/DC (Electric currents, Magnetic fields). The steady state equations of conservation of fluid mechanics, heat transfer and electromagnetics are developed by using the multiphysics couplings options available in the software. Compressible laminar flows with swirl are simulated for two plasma torch geometries, by assuming an artificial minimum value of 8000 S/m (σ_{min}) for the gas electrical conductivity. The computational results are then compared with experimental results of literature available for similar plasma torches.

Keywords: plasma torch, LTE, swirl, multiphysics, magneto-hydrodynamics equations.

1. Introduction

Plasma torches are used in processing of materials and in energy industry for producing plasma [1]. Direct currents (DC) arc plasma torches represent the primary components of thermal plasma processes (plasma spraying, metal welding and cutting, waste treatment, biogas production, etc.). In a non-transferred arc plasma torch, an electric arc can be glowed by applying a direct current (DC) between the cathode and the anode, then the plasma is obtained by heating, ionizing and expanding a working gas, introduced into the chamber. Due to the cooling of the anode, the gas close to the anode surface is cold, electrically no conductive, constricting the plasma.

The modeling of a DC plasma torch is cumbersome because of the presence of many simultaneous physical mechanisms [2], hence simplifications are required in order to obtain practical solutions. In the case of local thermodynamic equilibrium (LTE) hypothesis, the electrons and heavy particles temperatures are approximately equal and the plasma can be modeled by using the magneto-hydrodynamics (MHD) equations. However, the LTE approximation is not valid near the plasma boundaries, where the plasma may interact with refrigerated solid walls or cold gas streams. Since the plasma properties depend strongly on the temperature, an important deviation from the true plasma behavior is obtained when the electron temperature is restricted to be equal to the low heavy species temperature [2].

To reduce the complexity of the modeling work, stationary studies have been developed by many authors. However, this approach is not strictly correct, because the dynamic operating modes of the arc inside the torch (takeover and restrike modes) cannot be simulated. Only the steady operation mode, which leads to a rapid erosion of the anode torch in the proximity of the arc spot, can be represented and computed. Furthermore, in an axisymmetric two dimensional model, the arc spot is represented by a circumferentially uniform arc attachment, in some cases giving unrealistic behavior of the plasma [3]. Deng et *al.* [4] have proposed a MHD model to simulate the electromagnetic field, heat transfer and fluid flow in a DC torch under laminar and turbulent conditions. Mendoza et *al.* [5] modeled a DC thermal plasma torch using the same MHD equations of Deng et *al.* but in a three dimensional domain. By developing a parametric study of the inlet velocity in the torch, they were able to simulate the arc root attachment. Starting from the work of Deng *et al.* we developed in COMSOL Multiphysics® 5.1 a steady state two-dimensional model of a DC non- transferred arc plasma torch, under hypothesis of LTE [6,7].

In the present work, we apply our model to the plasma torch (*torch 1*) studied computationally by He-Ping Li (He-Ping Li *et al.* [3], He-Ping and Xi Chen [8]), and to the plasma torch (*torch 2*) used by Mozingo in an experimental activity [9]. The structure of the paper is the following. The description of the physical and mathematical model is given in Section 2, while Section 3 deals with the use of Comsol Multiphysics® to model the plasma torches. Finally, the computational results are presented in Section 4 and the conclusions in Section 5.

2. Model description and equations

2.1 Physical model

By applying axisymmetric conditions, the two DC plasma torches are modeled as a 2D region (Figs. 1 and 2). Argon (*torch 1*) and nitrogen (*torch 2*) are the working gas with physical properties obtained from the Comsol Multiphysics® material data base. We set specific free vortex flow regimes at the inlet by varying the intensity of the vortex and therefore of the azimuthal velocity v_θ. The anode and cathode are made up of copper. Due to the steady state

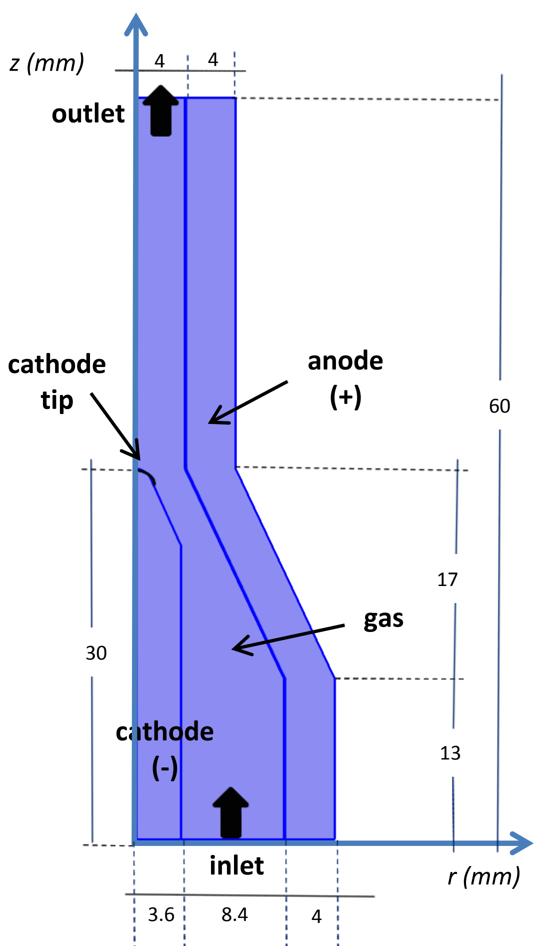

Figure 1. Schematic of the *torch 1* modeled by He-Ping Li [3, 8].

assumption, the arc´s reattachment processes on the anode surfaces is not modeled. For the radiation transfer mechanism in the torch, the plasma is considered optically thin and a net emission coefficient is used. Moreover, the gas flow is simplified by assuming a weakly compresible flow with a Mach number < 0.3. Gravity forces are not considered. Then, the plasma flow is studied by using the magnetohydrodynamics equations in the system of cylindrical coordinates *r*,*z*, shown in Figs. 1 and 2. In the model, we assume conditions of LTE, therefore the electrons and heavy particles temperatures are equal. In this case, a peculiar aspect is the low plasma electric conductivity σ for temperatures T below a critical value: for argon gas $\sigma \leq 1$ S/m if T< 4600 K, while for nitrogen gas $\sigma \leq 1$ S/m if T< 5300 K, approximately. Consequently, near the cooled anode wall of the torch, the electric current is not guaranteed. In order to ensure the electric flow, we use an artificial minimum value of 8000 S/m (σ_{min}) for the electrical conductivity of argon and nitrogen gases. In the literature, other authors

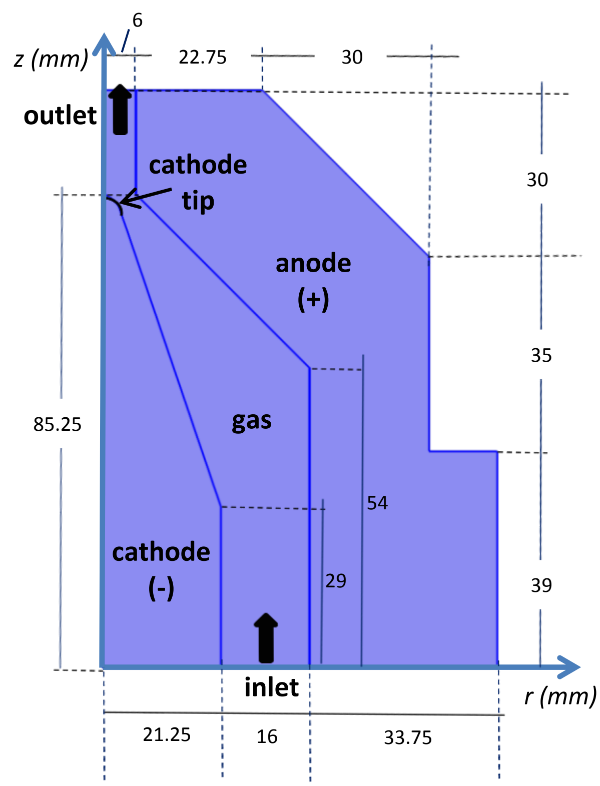

Figure 2. Schematic of the *torch 2* used by Mozingo [9].

[2, 3] have used similar methods near the anode walls. These approaches have been also used to predict the arc-root attachment position on the anode and the arc shape [3], as well as the arc reattachment in transient studies [2].

2.2 Mathematical model

For a steady state, laminar, weakly compressible gas flow, the continuity and momentum Navier-Stokes equations modeled in Comsol Multiphysics® are the following [10]:

$$\nabla \bullet (\rho \mathbf{u}) = 0 \quad (1)$$

$$\rho (\mathbf{u} \bullet \nabla)\mathbf{u} = \nabla \bullet [-p\mathbf{I} + \eta (\nabla \mathbf{u} + (\nabla \mathbf{u})^T) - \frac{2\eta}{3}(\nabla \bullet \mathbf{u})\mathbf{I}] + \mathbf{F} \quad (2)$$

In the above equations, the scalar magnitudes ρ and η are the fluid density and the dynamic viscosity, respectively. On the other hand, **u** is the fluid velocity, p is the pressure and **I** is the identity tensor. **F** represents the body forces, including the Lorentz force $\mathbf{F}_L$.

The conservation of the thermal energy in the torch is represented by the Fourier equation with convective terms and source terms [11]:

$$\rho C_p \mathbf{u} \nabla T = \nabla \bullet (k \nabla T) + Q \quad (3)$$

where T is the temperature, while k, C_p and Q, are the thermal conductivity, the specific heat capacity at constant pressure and the heat source, respectively. The term Q accounts for the Joule heating Q_J, the volumetric net radiation loss defined by a total volumetric emission coefficient and the enthalpy transport, which is the energy carried by the electric current.

For the stationary electromagnetic phenomena in the plasma torch, we use the definitions of the magnetic vector **A** and electric scalar V potentials:

$$\nabla \times \mathbf{A} = \mathbf{B} \quad (4)$$

$$\mathbf{E} = -\nabla V \quad (5)$$

where **B** is the magnetic flux density and **E** the electric field intensity. Consequently, the equations of Maxwell:

$$\nabla \times \mathbf{H} = \mathbf{J} \quad (6)$$

$$\nabla \times \mathbf{E} = \mathbf{0} \quad (7)$$

$$\nabla \bullet \mathbf{D} = 0 \quad (8)$$

$$\nabla \bullet \mathbf{B} = 0 \quad (9)$$

and the conservation of the charge:

$$\nabla \bullet \mathbf{J} = 0 \quad (10)$$

are formulated in terms of these potentials [12]. In the Maxwell equations, $\mathbf{J} = \sigma(\mathbf{E} + \mathbf{u} \times \mathbf{B})$ is the current density, $\mathbf{H} = \frac{1}{\mu}\mathbf{B}$ is the magnetic field intensity and $\mathbf{D} = \varepsilon \mathbf{E}$ is the electric flux density. Again **u** is the velocity field of the electromagnetic conductor, while the properties σ, μ and ϵ are the electric conductivity, magnetic permeability and electric permittivity of the material, respectively.

Additionally, in order to complete the thermo-fluid-electromagnetic coupled model of the plasma torch, the magnitude **F** and Q are expressed in terms of the electromagnetic variables **J**, **E** and **B**, by the definition of the terms:

$$\mathbf{F}_L = \mathbf{J} \times \mathbf{B} \quad (11)$$

$$Q_J = \mathbf{J} \bullet (\mathbf{E} + \mathbf{u} \times \mathbf{B}) \quad (12)$$

Eqs. 1 to 12 constitute the system of partial differential equations of the model, for which have to be defined boundary conditions.

3. Solution with Comsol Multiphysics®

The axisymmetric model of the DC arc plasma torches is implemented in Comsol Multiphisics® by using the physics of CFD (*Laminar flow)* [10], Heat Transfer (*Heat transfer in fluids/solids*) [11], AC/DC (*Electric currents, Magnetic fields*) [12] and Plasma *(Equilibrium Discharges Interface)* [13]. Also, the coupling phenomena of the plasma multiphysics flow in the DC torches are modeled by setting in Comsol Multiphysics®: plasma heat source (*electric→heat*), static current density component (*electric→magnetic*), induction current density (*magnetic→electric*), Lorentz forces (*magnetic →fluid flow*), boundary plasma heat source (rounded cathode tip) (*electric→ heat*), boundary plasma heat source (anode) (*electric→heat*), temperature couplings (*heat→electric*, *magnetic*, *fluid flow*).

At the inlet of the plasma torch, we set an argon flow rate G of 2.0 STP m^3/h for the *torch 1* of He-Ping Li [3, 8], giving approximately an axial velocity v_z of 1.35 m/s. Hence, defined the azimuthal velocity v_θ of the free vortex flow as $v_\theta = k_1 /r$, for the swirling inflow we consider the following three distinct values of k_1: 4.86x10$^{(-3)}$ m^2/s, 9.72x10$^{(-3)}$ m^2/s and 14.58x10$^{(-3)}$ m^2/s.

For the *torch 2* of Mozingo [9], who used nitrogen in its experiment, we assume a gas mass rate of 2.17 g/s, which corresponds approximately to 6.35 STP m^3/h and an inlet axial velocity of 1.37 m/s. Again, three free vortex flows at the inlet are modeled with k_1 equal to 0.291x10$^{(-1)}$ m^2/s, 0.582x10$^{(-1)}$ m^2/s and 0.873x10$^{(-1)}$ m^2/s, respectively.

For both the torches, we set a radial velocity v_r equal to 0. Finally, the other usual boundary conditions for the flow equations are no slip on the walls and pressure equal to zero at the outlet.

As boundary conditions for the thermal energy equation, we assume: temperature of 300 K at the inlet; an anode externally cooled ($h = 10^4$ W/(m^2 K) and T_{ext}= 500 K) and internally transferring energy by radiation (gray body); cathode tip with a temperature of 3500 K (thermionic emission); radiative heat transfer on the cathode walls (gray body); thermal insulation on the other surfaces of the torches. i.e. $-\mathbf{n} \bullet \mathbf{q} = 0$, where $\mathbf{q}$ is the heat flux and $\mathbf{n}$ is the normal direction.

To solve the Maxwell equations in terms of the potentials V and $\mathbf{A}$, we define the next values on the DC torches boundaries: a) on the rounded cathode tip, a normal current density J_n with values in the range of $10^7 \div 10^8$ A/m^2, equivalent to a current intensity I of 43.36÷433.6 A for the *torch 1*; a normal current density in the range of $10^6 \div 10^7$ A/m^2, which means a current intensity I of 50.38÷503.8 A for the *torch 2*; electric insulation, i.e. $\mathbf{n} \bullet \mathbf{J} = \mathbf{0}$, on the remaining surface of the cathode, at the inlet and outlet; grounded anode by fixing an electric potential of 0 V on the anode's outer surface; b) magnetic insulation in all the boundaries, with the magnetic potential $\mathbf{A}$ fulfilling the condition $\mathbf{n} \times \mathbf{A} = \mathbf{0}$ and a gauge fixing Ψ_0 = 1 A/m. Furthermore, we consider two cases of artificial minimum value of 8000 S/m (σ_{min}) for the electrical conductivity of the argon and nitrogen gases: a) σ_{min} = 8000 S/m in the whole fluid region; b) σ_{min} = 8000 S/m in a thin region between the cathode and anode.

Then, we specify the physical values for the electrodes of the plasma torch in the Equilibrium discharges interface. Both the cathode tip and copper anode wall are modeled as boundary plasma heat sources, mapping the electromagnetic surface losses as heat sources on the boundary. In this case, a surface work function of 4.15 V is the default value for copper electrodes in Comsol Multiphysics®.

Lastly, for all the equations we use a condition of axial symmetry on the z axis of the torch model.

The resulting system of partial differential equations is numerically solved in Comsol Multiphysics® 5.1 by dividing the 2D region of the torches in three different domains, i.e. cathode, fluid (plasma) and anode. Electric and magnetic fields are computed in the fluid and in the anode, the fluid flow is simulated only in the plasma, while the heat transfer equations are solved in the three regions. The computational domain is accomplished by meshing the *torch 1* with 1.1x10^5 triangle elements and the *torch 2* with 1.3x10^5 triangle elements and refining the discretization in the plasma region. The number of degrees of freedom to be solved for is nearly 1.4x10^6 for *torch 1* and 1.7x10^6 for *torch 2*. By using a fully coupled approach, the MUMPS direct solver is selected for numerically integrating the equations of the model. The computational model was run in a workstation with Intel Xenon CPU E5-2687W v2 16 cores, 3.40 GHz (2 processors), 216 GB RAM, 64bit and Windows 7 Operative System.

4. Results and discussion

Using the minimum value σ_{min} of 8000 S/m in the argon region, a normal current intensity of 0.8x10^8 A/m^2 in the cathode tip and a free swirling flow at the inlet with k_1 = 4.86x10$^{(-3)}$ m^2/s, Figs. 3 and 4 show the temperature and velocity fields of the *torch 1*, respectively. These fields are given in Figs. 5 and 6 for the *torch 2*, with the same σ_{min} in the nitrogen region, k_1= 0.291x10$^{(-1)}$ m^2/s and J_n= 0.7x10^7 A/m^2. Figs. 3 and 5 reveal the arc column of gas that, introduced into the chamber of the torch upstream of the cathode, is heated, ionized and expanded by the Joule heating effect of Eq. 12. On the other hand, Figs. 4 and 6 show the velocity distribution resulting from both the gas expansion and acceleration, the latter one due to

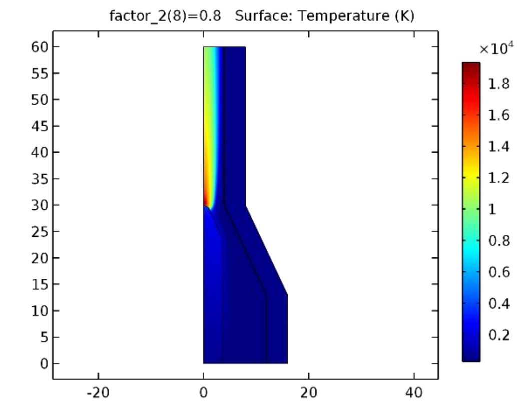

Figure 3. Temperature field of the *torch 1* (G = 2.0 STP m^3/h, k_1 = 4.86x$10^{(-3)}$ m^2/s, J_n= 0.8x10^8 A/m^2).

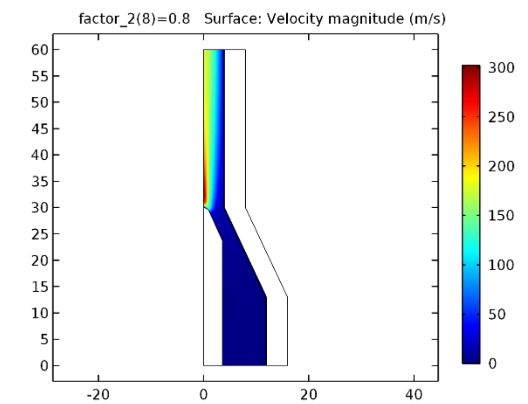

Figure 4. Velocity field of the *torch 1* (G = 2.0 STP m^3/h, k_1 = 4.86x$10^{(-3)}$ m^2/s, 0.8x10^8 A/m^2).

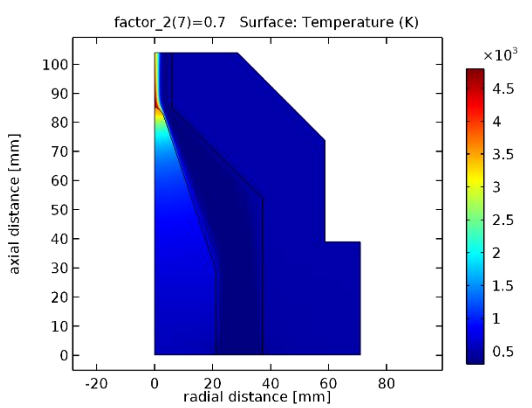

Figure 5. Temperature field of the *torch 2* (G = 6.35 STP m^3/h, k_1 = 0.291x$10^{(-1)}$ m^2/s, J_n= 0.7x10^7 A/m^2).

the Lorentz force $\mathbf{F}_L$ acting over the electrically charged gas. According to Eq. 11, $\mathbf{F}_L$ depends on the cross product of the fields **J** and **B**, which is higher in the fluid region behind the cathode tip.

He-Ping and Xi Chen [8] studied the *torch 1*

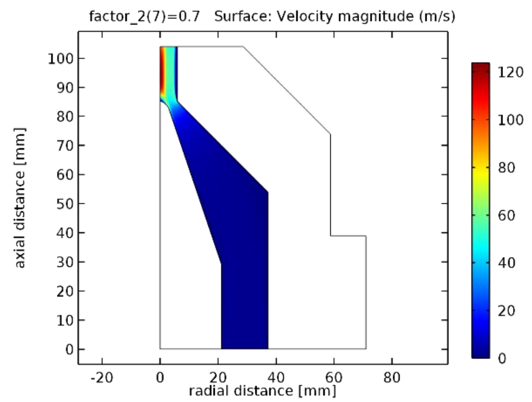

Figure 6. Velocity field of the *torch 2* (G = 6.35 STP m^3/h, k_1 = 0.291x$10^{(-1)}$ m^2/s, J_n= 0.7x10^7 A/m^2).

under similar conditions by developing bi- and three-dimensional models. The 2D results showed that the highest temperature is located at the torch axis, as in Fig. 3, whereas the 3D simulations predicted a non-axisymmetric temperature field, with the highest temperature at an off-axis position. The maximum temperature and axial velocity within the torch, computed by He-Ping and Xi-Chen, were higher than the ones obtained by our simulations. These differences might be due to the three-dimensional pattern of the plasma flow and the artificial electrical conductivity used in the model. The position of the arc attachment, predicted by He-Ping and Xi Chen, is near the intersection between the convergent part and the cylindrical part of the anode (z=30 mm) and it is not uniform in the circumferential direction. The same position of z=30 mm is given by our computational results. For *torch 1* in Fig. 7 and *torch 2* in Fig. 8, we plot the current density normal to the anode wall. In these figures, the maximum current density would correspond to the arc root attachment at the inner anode walls. For the two torches, the arc root is located exactly at the intersection between the cone and the upper cylinder, which is z=30 mm for *torch 1* and z=85.25 mm for *torch 2*.

A second simulation, with an artificial σ_{min} only in a narrow region between the cathode and anode, is carried out for investigating the possible dependence of the computational results on the gas electrical conductivity used in the model. In another work [3], He-Ping Li *et al*. had applied the Steenbecks's minimum principle and computed the arc-root attachment at a distance z=36 mm for the same *torch 1*, using a current of 400 A and an

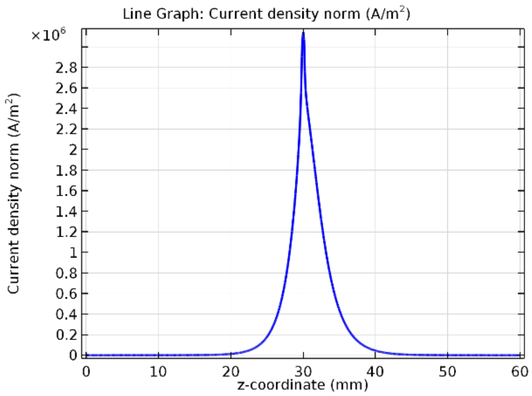

Figure 7. Current density norm at the internal anode wall of *torch 1* (G= 2.0 STP m^3/h, k_1 = 4.86x10$^{(-3)}$ m^2/s, J_n= 0.8x10^8 A/m^2).

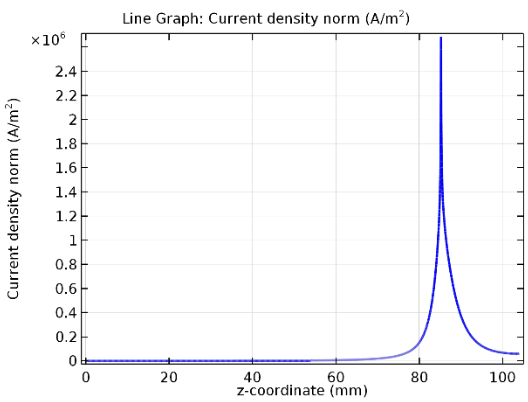

Figure 8. Current density norm at the internal anode wall of *torch 2* (**G** = 6.35 STP m^3/h, k_1 = 0.291x10$^{(-1)}$ m^2/s, J_n= 0.7x10^7 A/m^2).

argon gas flow rate of 2.0 STP m^3/h. Therefore, we locate a thin channel between the central region of the torch and the anode wall in correspondence of this axial distance and apply there the condition of σ_{min}= 8000 S/m. This is equivalent to fix the arc-root attachment at z=36 mm, as the plot of Fig. 9 highlights. In the simulation, the current density norm at the internal anode wall of *torch 1* has been computed for G = 2.0 STP m^3/h, k_1 = 4.86x10$^{(-3)}$ m^2/s and J_n= 0.4x10^8 A/m^2 (I=173.4 A). Then, the new temperature and velocity fields of *torch 1* are depicted in the Figs. 10 and 11, respectively. Even with a smaller value of the normal current density in the cathode tip, from these plots we gather that the maximum temperature is now the same of the previous case of Fig. 3, whereas the axial velocity

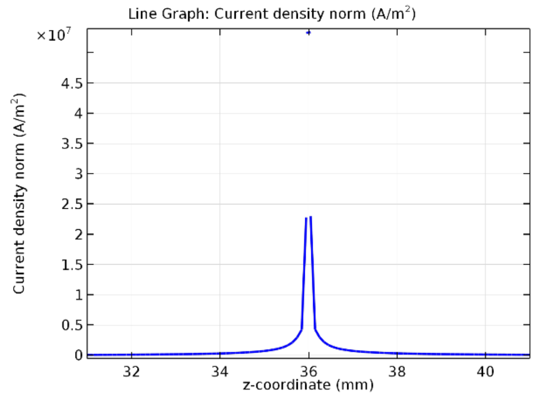

Figure 9. Current density norm at the internal anode wall of *torch 1*, fixing the arc-root attachment (G = 2.0 STP m^3/h, k_1 = 4.86x10$^{(-3)}$ m^2/s, J_n= 0.4x10^8 A/m^2).

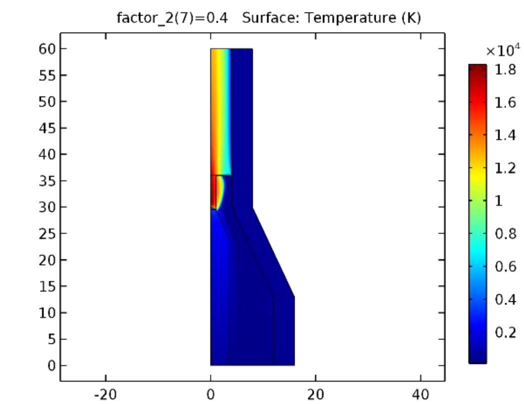

Figure 10. Temperature field of the *torch 1*, fixing the arc-root attachment (G = 2.0 STP m^3/h, k_1 = 4.86x10$^{(-3)}$ m^2/s, J_n= 0.4x10^8 A/m^2).

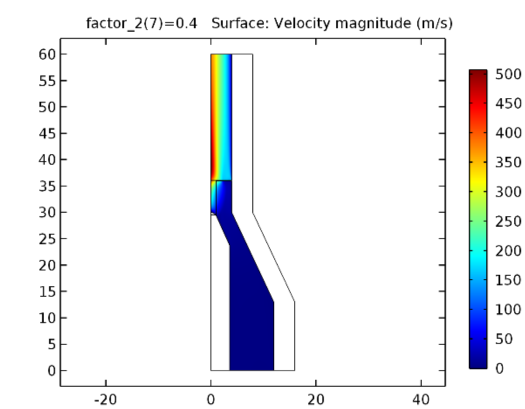

Figure 11. Velocity field of the *torch 1*, fixing the arc-root attachment (G = 2.0 STP m^3/h, k_1 = 4.86x10$^{(-3)}$ m^2/s, 0.4x10^8 A/m^2).

is nearly doubled. Therefore, by using the σ_{min} in a smaller region, the maximum temperature and axial velocity values within the torch result to be closer to the ones calculated by He-Ping Li *et al*. [3].

5. Conclusions

Two geometries of DC plasma torches have been modeled and the associated plasma flows simulated, by developing a 2D axisymmetric model of laminar flow and heat transfer, coupled to the electromagnetic field. In order to solve the partial differential equations of electric currents and magnetic fields, both in the gas and in the anode region, we have applied appropriate boundary conditions in the modeling work. Lorentz forces and Joule heating effects have been modeled, coupled to the physical model of the plasma torch and finally computed. In order to ensure the electric flow, we have used an artificial minimum value of 8000 S/m (σ_{min}) for the electrical conductivity of the gas. The numerical results of the gas temperature and axial velocity result to be quite satisfactory, although more complete reproductions of the thermal and fluid phenomena might be obtained with three-dimensional modelling. In that case, computational requirements and computing times should be also taken into account for.

6. References

[1] M. I . Boulos, P. Fauchais, and E. Pfender, *Thermal Plasmas: Fundamentals and Applications*, Plenum Press, New York, (1994).

[2] J.P. Trelles, C. Chazelas, A. Vardelle, and J.V.R. Heberlein, *Arc plasm torch modeling*, Journal of Thermal Spray Technology, **18**, No. 5/6, 728-752, (2009).

[3] He-Ping Li, E. Pfender and Xi Chen, *Application of Steenbeck's minimum principle for three dimensional modelling of DC arc plasma torches*, Journal of Physics D: Applied Physics, **36**, 1084-1096, (2003).

[4] Deng Jing, Li Yahojian, Xu Yongxiang and Sheng Hongzhi, *Numerical simulation of fluid flow and heat transfer in a DC non-transferred arc plasm torch operating under laminar and turbulent conditions*, Plasma Science and Technology, **13**, vol. 2, 201-207, (2011).

[5] N.Y. Mendoza Gonzalez, L. Rao, P. Carabin, A. Kaldas and J.L. Meunier, A *three-dimensional model of a DC thermal plasma torch for waste treatment applications*, International Symposium on Plasma Chemistry ISPC-19, July 27-31, 2009, Bochum, Germany.

[6] B. Chiné, M. Mata and I. Vargas, *Modeling a DC plasma with Comsol Multiphysics*, Comsol Conference 2015, October 14-16 2015, Grenoble, France.

[7] B. Chiné, *A 2D Model of a DC Plasma Torch*, Comsol Conference 2016, October 12-14 2016, Munich, Germany.

[8] He-Ping Li and Xi Chen, *Three-dimensional modelling of a dc non-transferred arc plasma torch*, Journal of Physics D: Applied Physics, **34**, L99-L102, (2001).

[9] J.A. Mozingo, *Evaluation of a strut-plasma torch combination as a supersoni igniter-flameholder*, MSc. Thesis, Virginia Polytechnic Institute and State University, Blacksburg, Virginia, USA, (2004).

[10] Comsol AB, *Comsol Multiphysics-CFD Module*, User's Guide, Version 5.1, (2015).

[11] Comsol AB, *Comsol Multiphysics-Heat Transfer Module*, User's Guide, Version 5.1, (2015).

[12] Comsol AB, *Comsol Multiphysics-AC/DC Module, User's Guide*, Version 5.1, (2015).

[13] Comsol AB, *Comsol Multiphysics-Plasma Module, User's Guide*, Version 5.1, (2015).

7. Acknowledgements

The author gratefully acknowledges the financial aid provided by the Vicerrectoria de Investigaciòn y Extensiòn of the Instituto Tecnològico de Costa Rica, through the project 5401-1490-2001.